Journal of Alloys and Compounds 506 (2010) 533–536

Contents lists available at ScienceDirect

Journal of Alloys and Compounds

journal homepage: www.elsevier.com/locate/jallcom

Magnetic and magnetostrictive properties in high-pressure synthesized $Dy_{1-x}Pr_xFe_{1.9}(0 \le x \le 1)$ cubic Laves alloys

Y.G. Shi [a,*], S.L. Tang [b], L.Y. Lv [b], J.Y. Fan [a]

[a] Department of Applied Physics, Nanjing University of Aeronautics and Astronautics, Nanjing 210016, China
[b] National Laboratory of Solid State Microstructures, Nanjing University, Nanjing 210093, China

ARTICLE INFO

Article history:
Received 30 May 2010
Received in revised form 13 July 2010
Accepted 15 July 2010
Available online 22 July 2010

PACS:
75.50.Bb
75.80.+q

Keywords:
Rare-earth compounds
High-pressure annealing
Magnetic properties
Magnetostriction

ABSTRACT

Polycrystalline alloys $Dy_{1-x}Pr_xFe_{1.9}$ $(0 \le x \le 1)$ were synthesized by arc-melting and subsequent high-pressure annealing. Their crystal structure, magnetic properties and magnetostriction have been investigated. X-ray diffraction results show that the system exhibits almost single cubic Laves phase with $MgCu_2$-type structure over the whole range. The lattice parameter of the cubic Laves phase increases linearly with increasing Pr concentration, while the Curie temperature goes the opposite way. The saturation magnetization for $Dy_{1-x}Pr_xFe_{1.9}$ decreases with the increase of x and reaches a minimum at $x = 0.4$, then it continues to increase with further increase of x, which reflects the antiparallel magnetic moment of Dy and Pr. The magnetostriction $\lambda_{||} - \lambda_{\perp}$ first increases and then decreases within the range of $0.0 \le x \le 0.4$, and increases monotonically with further increasing x.

1. Introduction

Studies on C15 cubic Laves phases $REFe_2$ (RE = rare earths) alloys are of great importance due to their potential applications as magnetostrictive materials in sonar transducers, sensors, actuators, etc. According to the single-ion model [1], $PrFe_2$ should have a larger calculated magnetostriction than $TbFe_2$ and $DyFe_2$, which is ascribed to the large second-order Stevens' factor α_J, ground state angular momentum J and average radius squared $\langle r_{4f}^2 \rangle$ of the 4*f* electron shell of the Pr^{3+} ion. In addition, due to its low price, a magnetostrictive compound with high-Pr concentration should be of more practical value. Accordingly, much attention has been paid to magnetostrictive alloys with Pr [2–6]. However, former studies showed that the alloy with cubic Laves phase is difficult to be synthesized under normal pressure when the concentration of Pr is high. For example, Wang et al. investigated the structure and magnetostriction of normal-pressure annealed $Dy_{1-x}Pr_xFe_2$ alloys [7]. It was found that $(Pr,Dy)Fe_2$ cubic Laves phase is the main phase of the alloy with $x \le 0.2$. Nevertheless, $(Pr,Dy)Fe_3$ or $(Pr,Dy)_2Fe_{17}$ becomes the main phases when $x > 0.2$. Ren et al. found that the introduction of a small amount of boron is beneficial to the formation of high-Pr content cubic Laves phase [8,9]. However, the single cubic Laves phase could not be synthesized in $Dy_{1-x}Pr_x(Fe_{0.9}B_{0.1})_2$ alloys when Pr concentration exceeds 40 at.% in rare-earth sublattice. Up to present, $Dy_{1-x}Pr_xFe_2$ cubic Laves alloys with high-Pr content have not yet been synthesized and their magnetic properties remain unknown. Recently, we reported that the structure and magnetic properties of high-pressure synthesized $PrFe_x$ $(1.5 \le x \le 3.0)$ alloys and the single cubic Laves phase was realized in $PrFe_{1.9}$ [10]. In this paper, polycrystalline alloys $Dy_{1-x}Pr_xFe_{1.9}$ $(0 \le x \le 1)$ with cubic Laves phase have been successfully synthesized by a method of arc-melting and subsequent high-pressure annealing. The crystal structure, magnetic properties and the magnetostriction of the alloys are investigated.

2. Experimental

Ingots with stoichiometric composition of $Dy_{1-x}Pr_xFe_{1.9}$ ($x = 0.0$, 0.2, 0.4, 0.6, 0.7, 0.8, 0.9, and 1.0) were prepared by melting the constituent metals in a magneto-controlled arc furnace under a high-purity argon atmosphere. The purity of constituents is 99.9% for Pr and Dy, and 99.8% for Fe. During the arc-melting process, a variable magnetic field was applied to control the focus of the arc and stir the liquids, so that the samples can be melted thoroughly and homogeneously. The ingot (about 1 g for each sample) was pressed into disk and wrapped in tantalum foils, then, it was loaded into a graphite pipe heater with the shape of cylinder. Pyrophyllite was used for outside layers of pressure transmitting layer and MgO as the inner one. The schematic diagram of the sample assembly for high-pressure annealing is shown in Fig. 1. The assembly was pressed to 6 GPa by a hexahedral anvil press and heated to 900 °C for 30 min. Conventional X-ray diffraction (XRD)

* Corresponding author.
E-mail address: shiyangguang@gmail.com (Y.G. Shi).

0925-8388/$ – see front matter © 2010 Elsevier B.V. All rights reserved.
doi:10.1016/j.jallcom.2010.07.117

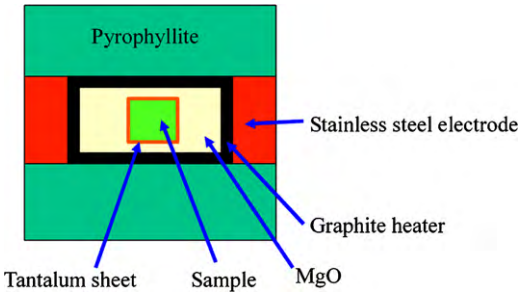

Fig. 1. The schematic diagram of the sample assembly for high-pressure annealing.

analysis was carried out using Cu Kα radiation with a Rigaku D/Max-gA diffractometer. The XRD data were analyzed using the Jade 5.0 XRD analytical software (Materials Data, Inc., Livemore, CA). The Curie temperature was detected by a thermal gravitation analyzer with a vertical gradient magnetic field under the samples. The magnetization at room temperature of the compounds was measured using a superconducting quantum interference device magnetometer at fields up to 50 kOe. The shape of sample for magnetostriction measurement was mainly cylindrical with a diameter of 10 mm and a height of 2 mm. The linear magnetostriction of the sample was measured using standard strain-gauge technique in directions parallel ($\lambda_{||}$) or perpendicular ($\lambda_{\perp}$) to applied magnetic fields up to 10 kOe at room temperature.

3. Results and discussion

The XRD patterns for $Dy_{1-x}Pr_xFe_{1.9}$ with different Pr concentrations are shown in Fig. 2. It can be seen that the system exhibits almost single cubic Laves phase with $MgCu_2$-type structure over the whole range, coexisting with a minor of impurities, i.e. rear-earth phases. In comparison with the structure of $Dy_{1-x}Pr_xFe_2$ [7] and $Dy_{1-x}Pr_x(Fe_{0.9}B_{0.1})_2$ [8] alloys with high-Pr content prepared by normal-pressure annealing, our samples are free of RE_2Fe_{17} or $REFe_3$ phase. Generally, the atomic size plays an important role in the formation $REFe_2$ cubic Laves alloys. It can be estimated that the ideal radius ratio between RE and Fe for a cubic Laves phase is 1.225 [11]. Among all the Lanthanide elements, Pr is the largest atom except Ce. Due to the mixed-valence behavior of Ce, $CeFe_2$ cubic Laves phase can be easily synthesized at ambient pressure [12]. But $PrFe_{1.9}$ cubic Laves phase could not be synthesized due to the large radius ratio between Pr and Fe. On the other hand, $PrFe_{1.9}$ with

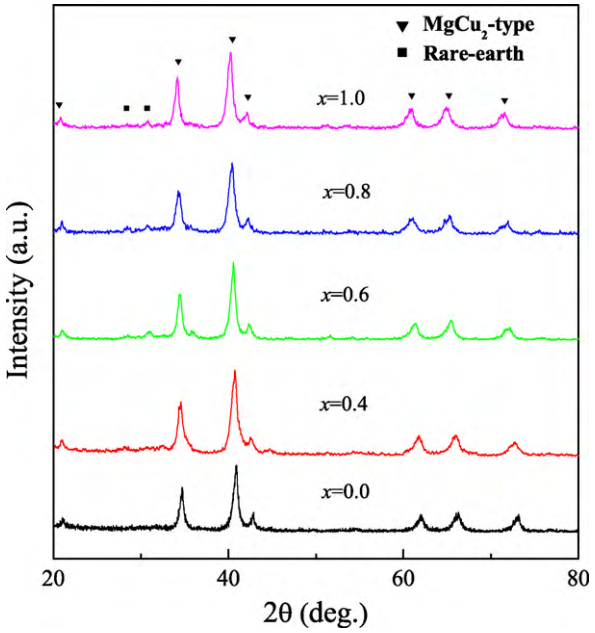

Fig. 2. The XRD patterns for $Dy_{1-x}Pr_xFe_{1.9}$ with different Pr concentrations.

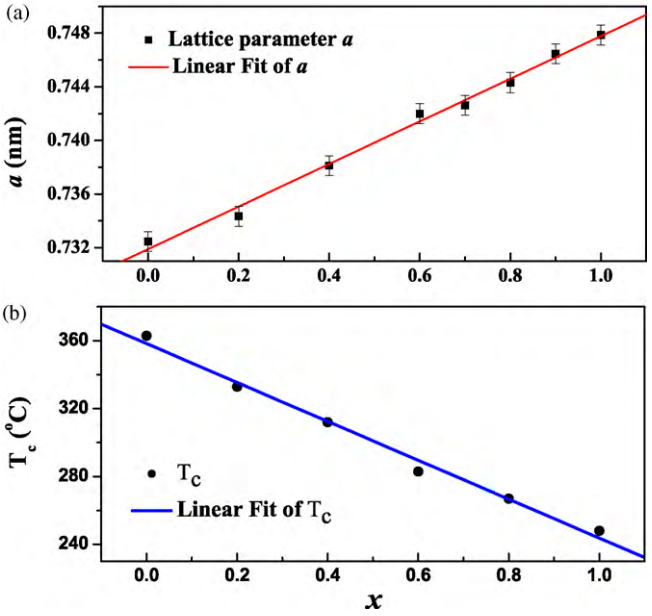

Fig. 3. (a) The lattice parameter a and (b) the Curie temperatures T_c of $Dy_{1-x}Pr_xFe_{1.9}$ cubic Laves phase as a function of Pr concentration.

Table 1
Lattice parameter a (nm), Curie temperature T_c (°C), magnetization σ_{max} (emu/g) at a magnetic field of 50 kOe, coercivity $_iH_c$ (Oe) at 300 K, and magnetostriction $(\lambda_{||}-\lambda_{\perp})_{max}$ (ppm) at a magnetic field of 10 kOe at room temperature for $Dy_{1-x}Pr_xFe_{1.9}$ cubic Laves phase compounds.

Sample	a	T_c	σ_{max}	$_iH_c$	$(\lambda_{||}-\lambda_{\perp})_{max}$
0.0	0.7324(5)	363	86	364	311
0.2	0.7343(4)	333	44	456	372
0.4	0.7381(2)	312	23	913	255
0.6	0.7419(9)	283	26	600	462
0.8	0.7443(2)	267	56	110	743
1.0	0.7478(7)	248	88	50	984

$MgCu_2$-type structure has been proved to be a metastable phase and its decomposition temperature is as low as 408 °C [10]. These may be the reasons that preclude the ambient pressure synthesis of the $Dy_{1-x}Pr_xFe_{1.9}$ cubic Laves alloys when the Pr concentration exceeds 0.2. Therefore, the formation of $Dy_{1-x}Pr_xFe_{1.9}$ cubic Laves phase with high-Pr concentration should be ascribed to the effects of high pressure.

The lattice parameter (a) of $Dy_{1-x}Pr_xFe_{1.9}$ Laves phase is shown in Fig. 3(a), also listed in Table 1. An approximate linear increase with Pr concentration from 0.0 to 1.0 is found, as expected from Vegard's law: $a = xa_1 + (1-x)a_2$, where a_1 and a_2 are the lattice parameters of $PrFe_{1.9}$ and $DyFe_{1.9}$, respectively. The lattice parameter of $PrFe_{1.9}$ is up to 0.7478 nm, which is the largest one among the $REFe_2$ alloys [1,13]. The increase of lattice parameter with increasing Pr concentration is due to the larger ionic radius Pr^{3+} than that of Dy^{3+}. The Curie temperature of $Dy_{1-x}Pr_xFe_{1.9}$ cubic Laves phase is shown in Fig. 3(b). It can be seen that the Curie temperature decreases almost linearly from 363 °C ($DyFe_{1.9}$) to 248 °C ($PrFe_{1.9}$). In general, the Curie temperature is determined by the exchange of 3*d*–3*d* atoms and modulated by 3*d*–4*f* hybridization [14]. As for $Dy_{1-x}Pr_xFe_{1.9}$ alloys, the increasing of the Curie temperature indicates that the 3*d*–4*f* coupling becomes weak with increasing Pr concentration.

The hysteresis loops measured at 300 K for $Dy_{1-x}Pr_xFe_{1.9}$ alloys are shown in Fig. 4. The inset of Fig. 4 shows the initial magnetization curves at the same temperature. We can note that the magnetization of the alloys is close to saturation at the field of 50 kOe. The magnetization σ_{max} at 50 kOe and the coercivity $_iH_c$

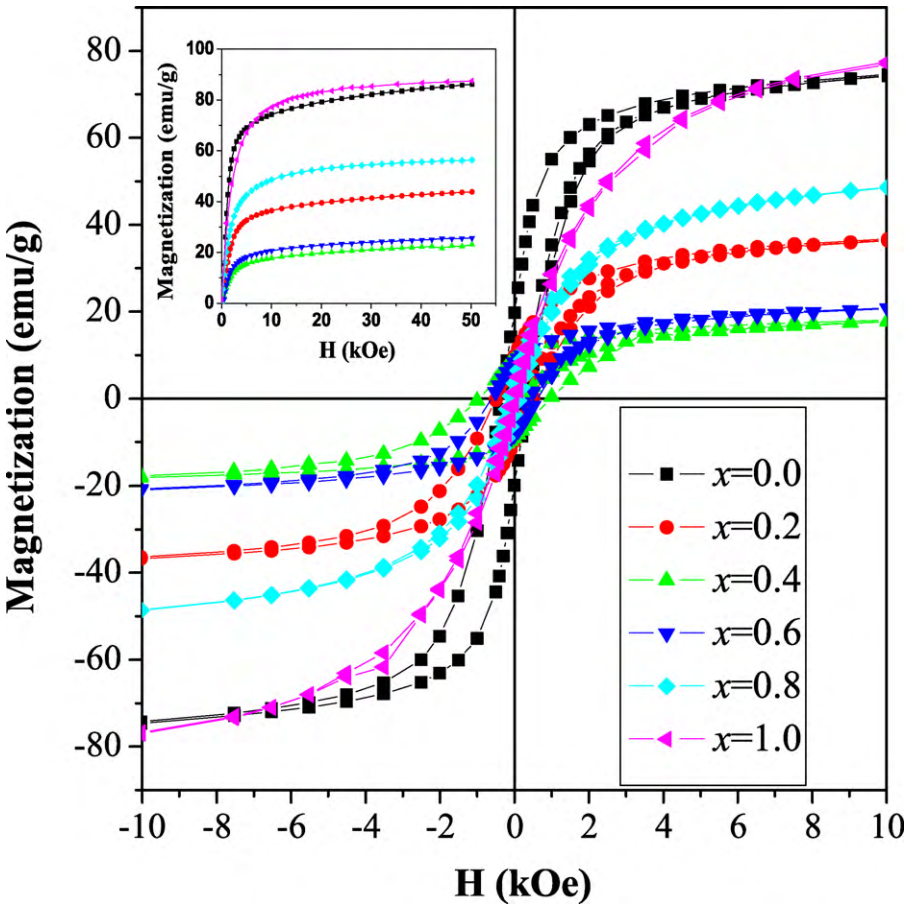

Fig. 4. Hysteresis loop of $Dy_{1-x}Pr_xFe_{1.9}$ alloys at 300 K. The inset shows the initial curve of $Dy_{1-x}Pr_xFe_{1.9}$ up to 50 kOe.

of $Dy_{1-x}Pr_xFe_{1.9}$ are summarized in Table 1. For clarity, σ_{max} as a function of Pr concentration is also plotted in the Fig. 5. It can be seen that σ_{max} decreases with increasing Pr concentration to a minimum at $x = 0.4$ and then increases with further increasing x. This can be understood by the compensation of sublattice magnetization: the moment of light rare-earth Pr is parallel to that of Fe whereas the moment of heavy rare-earth Dy is unparallel to. The magnetic moment of $Dy_{1-x}Pr_xFe_{1.9}$ can be described as: $\mu_s = (1-x)\mu_{Dy} - 1.9\,\mu_{Fe} - x\mu_{Pr}$. As a result, the competition between these two sublattice moments leads to first decrease and following increase in the total net magnetization. From the analysis the magnetization of the alloy system, we can also get a conclusion that the magnetic moment compensation point between Dy and Pr should be within the range of $0.4 \le x \le 0.6$ at 300 K. The coercivity ${}_iH_c$ of $Dy_{1-x}Pr_xFe_{1.9}$ as a function of Pr concentration is also presented in Fig. 5. With increasing the concentration of Pr, ${}_iH_c$ increases from 364 Oe ($DyFe_{1.9}$) to 913 Oe ($Dy_{0.6}Pr_{0.4}Fe_{1.9}$) and following decreases to 50 Oe ($PrFe_{1.9}$).The ${}_iH_c$ of $DyFe_{1.9}$ is much larger than $PrFe_{1.9}$, which implies the lower anisotropy of $PrFe_{1.9}$ than that of $DyFe_{1.9}$ [9]. $Dy_{0.6}Pr_{0.4}Fe_{1.9}$ possesses the lowest saturation magnetization and the largest coercivity among the present system.

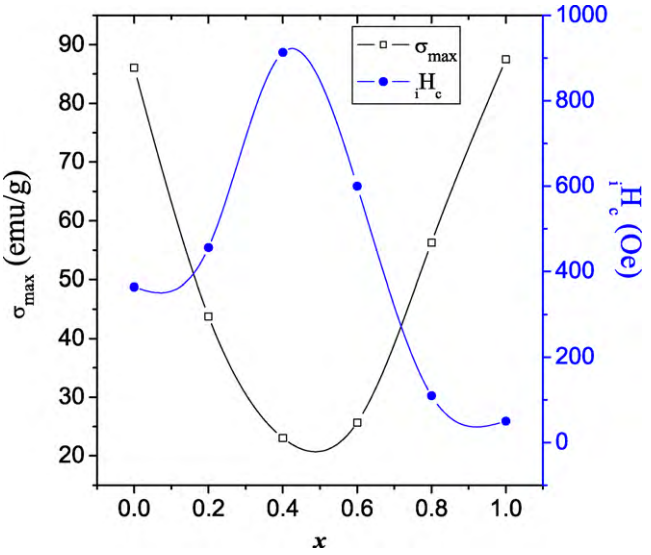

Fig. 5. The magnetization σ_{max} at 50 kOe and the coercivity ${}_iH_c$ of $Dy_{1-x}Pr_xFe_{1.9}$ alloys at 300 K.

Fig. 6(a) shows the magnetostriction $(\lambda_{||} - \lambda_{\perp})$ of $Dy_{1-x}Pr_xFe_{1.9}$ versus the applied field at room temperature. It is obvious that $DyFe_{1.9}$ possesses a much lower magnetostriction than $PrFe_{1.9}$. This might be ascribed to the different room-temperature easy magnetization directions (EMD) of these two alloys. The EMD of $PrFe_{1.9}$ lies along ⟨1 1 1⟩ [10,15], while that of $DyFe_{1.9}$ is ⟨1 0 0⟩ [1]. According to the atomic model for anisotropic magnetostriction proposed by Callen and Clark [1], a large rhombohedral distortion is allowed when the EMD of $REFe_2$ lies along ⟨1 1 1⟩. Conversely, only small distortions are permitted when alloy's EMD is along ⟨1 0 0⟩. Besides, we can see that the magnetostriction of $DyFe_{1.9}$ is much harder to get saturation than that of $PrFe_{1.9}$. This can be well understood since $DyFe_{1.9}$ has larger anisotropy than $PrFe_{1.9}$.

In order to investigate the variation of magnetostriction with different Pr concentrations, the magnetostriction $\lambda_{||} - \lambda_{\perp}$ as a func-

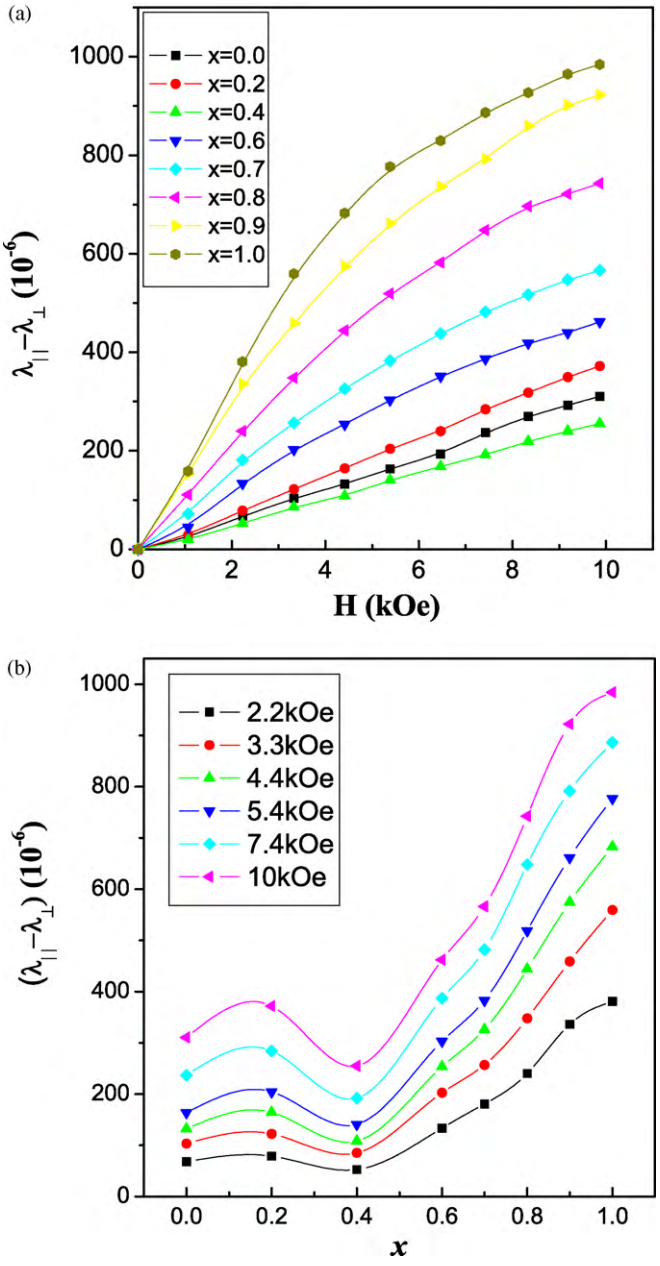

Fig. 6. (a) The room-temperature magnetostriction ($\lambda_{||} - \lambda_{\perp}$) of $Dy_{1-x}Pr_xFe_{1.9}$ versus the applied field. (b) The magnetostriction ($\lambda_{||} - \lambda_{\perp}$) as a function of Pr concentration.

tion of x is plotted in Fig. 6(b). The magnetostriction increases with the addition of Pr and shows a maximum around $x = 0.2$. This tendency is similar to that of $Dy_{1-x}Pr_x(Fe_{0.9}B_{0.1})_2$ system with $0.0 \le x \le 0.3$ [8]. With further increasing x to 0.4, the magnetostriction exhibits a minimum. This can be explained by single-ion model [16]: the saturation magnetostriction is proportional to M_{SR}^3, where M_{SR} is the saturation magnetization of the rare-earth sublattice; since the average of M_{SR} is the lowest at $x = 0.4$, the magnetostriction ($\lambda_{||} - \lambda_{\perp}$) should also show a minimum value. A similar behavior can also be found in some other heavy rare-earth and light rare-earth mixed pseudobinary alloys, such as $Tb_{0.6}Pr_{0.4}Fe_{1.9}$ [17] and $Tb_{0.6}Nd_{0.4}Fe_{1.9}$ [18]. With x increasing from 0.4 to 1.0, the magnetostriction of the system increases monotonically, which should be ascribed to the larger magnetostriction of $PrFe_{1.9}$ than that of $DyFe_{1.9}$.

4. Conclusion

The magnetic properties and the magnetostriction of $Dy_{1-x}Pr_xFe_{1.9}$ alloy system have been investigated in detail. The method of high-pressure annealing can break through the solubility limitation of Pr in $Dy_{1-x}Pr_xFe_{1.9}$ cubic Laves alloys. The decrease of Curie temperature with increasing Pr can be associated with the decreasing strength of $3d$–$4f$ coupling. The variation of saturation magnetization for $Dy_{1-x}Pr_xFe_{1.9}$ is ascribed to the antiparallel moments between Dy and Pr. $PrFe_{1.9}$ possesses a much larger magnetostriction than $DyFe_{1.9}$. The magnetostriction is not linearly increases with increasing x, but presents a minimum at $x = 0.4$. The magnetostriction behavior of $Dy_{0.6}Pr_{0.4}Fe_{1.9}$ can be understood on the basis of single-ion model.

Acknowledgments

This work is supported by Natural Science Foundation of China (Grant Nos. 50771055 and 50831006) and National Key Project of Fundamental Research of China (Grant No. 2005CB623605).

References

[1] A.E. Clark, in: E.P. Wohlfarth (Ed.), Ferromagnetic Materials, vol. 1, North-Holland, Amsterdam, 1980, pp. 531–589.
[2] Z.J. Guo, B.W. Wang, Z.D. Zhang, X.G. Zhao, X.M. Jin, W. Liu, Q.F. Xiao, Appl. Phys. Lett. 71 (1997) 2836.
[3] Y.X. Li, C.C. Tang, J. Du, G.G. Wu, W.S. Zhan, W.L. Yan, G.Z. Xu, Q.X. Yang, J. Appl. Phys. 83 (1998) 7753.
[4] J.J. Liu, D.K. Xiong, W.J. Ren, Z.D. Zhang, S.W. Or, J. Alloys Compd. 427 (2007) 271.
[5] J.J. Liu, P.Z. Si, W.S. Zhang, X.C. Liu, J. Alloys Compd. 474 (2009) 9.
[6] F. Yang, W. Liu, S.Q. Li, X.K. Lv, J. Li, Z.D. Zhang, Mater. Lett. 64 (2010) 608.
[7] B.W. Wang, Z.J. Guo, Z.D. Zhang, X.G. Zhao, S.C. Busbridge, J. Appl. Phys. 85 (1999) 2805.
[8] W.J. Ren, Z.D. Zhang, X.G. Zhao, C.Y. You, D.Y. Geng, J. Alloys Compd. 359 (2003) 119.
[9] W.J. Ren, Z.D. Zhang, X.P. Song, X.G. Zhao, X.M. Jin, Appl. Phys. Lett. 82 (2003) 2664.
[10] Y.G. Shi, S.L. Tang, Y.J. Huang, B. Nie, B. Qian, L.Y. Lv, Y.W. Du, J. Alloys Compd. 443 (2007) 11.
[11] D. Thoma, J. Perepezko, J. Alloys Compd. 224 (1995) 330.
[12] C.C. Tang, W.S. Zhan, Y.X. Li, D.F. Chen, J. Du, G.H. Wu, J.Y. Li, K.C. Jia, J. Phys. Condens. Matter 9 (1997) 9651.
[13] J.F. Cannon, D.L. Robertson, H.T. Hall, Mater. Res. Bull. 7 (1972) 5.
[14] K.H.J. Buschow, Rep. Prog. Phys. 40 (1977) 1192.
[15] M. Shimotomai, H. Miyake, M. Doyama, J. Phys. F. 10 (1980) 707.
[16] E. Callen, H.B. Callen, Phys. Rev. 139 (1965) A455.
[17] Y.G. Shi, S.L. Tang, R.L. Wang, H.L. Su, Z.D. Han, L.Y. Lv, Y.W. Du, Appl. Phys. Lett. 89 (2006) 202503.
[18] Y.G. Shi, S.L. Tang, Y.J. Huang, L.Y. Lv, Y.W. Du, Appl. Phys. Lett. 90 (2007) 142515.